

Accurate modeling of periodic and graded multilayer X-ray scattering from surface microroughness characterization

B. Salmaso¹, D. Spiga¹, R. Canestrari¹, L. Raimondi^{1,2}

¹*INAF/Brera Astronomical Observatory, Via E. Bianchi 46, 23807 Merate (LC), Italy*

²*Università degli Studi dell'Insubria, Via Valleggio 11, 22100 Como (CO), Italy*

ABSTRACT

Several hard X-ray imaging telescopes of the next future will be characterized by a high angular resolution. To this end, it is necessary to produce optics with a very low surface microroughness, as this is responsible of X-ray scattering, which results in image quality degradation especially at the higher energies. To the smooth surface approximation, it is possible to compute the X-Ray Scattering (XRS) from the Power Spectral Density (PSD) of the surface roughness. Indeed, multilayers coatings will be used to reflect X-rays beyond 10 keV; in this case the scattering pattern is more complicated but it can still be computed from the PSDs of each interface and the cross-correlation functions of the rough profiles. A growth model able to describe the roughness evolution of the surfaces enables us to compute the XRS of the multilayer, which can be directly compared to the experimental data. With this approach we aim to validate the roughening model assumed and to accurately predict the scattering pattern we expect on the focal plane. In this work we show the application of this formalism: direct measurements of the PSDs for the substrate and the outermost layer of a multilayer sample are used as input for the code to model the PSD growth. XRS measurements of that sample, performed at the energy of 8.05 keV, are presented to validate the modeling achieved.

Keywords: multilayer coatings, microroughness, Power Spectral Density, X-Ray Scattering

1. INTRODUCTION

X-ray telescopes equipped with imaging optics will use multilayer coatings to enhance their reflectivity. The surface of the mirrors, however, is unavoidably affected by some surface roughness that degrades the reflectivity and increases the X-ray scattering (XRS). This, in turn, entails a degradation of the angular resolution, with effects increasing with the energy of X-rays, in addition to the aberrations caused by profile errors. In order to compute the XRS from the Power Spectral Density (PSD) of the surface roughness, the perturbation theory, in the smooth surface approximation, is used in general. For a single rough surface, the relation between XRS and PSD is a simple, well-known proportionality^{1,2}; in contrast, for a multilayer film, the scattering arises from the interference of X-rays scattered by several interfaces^{3,4}. Therefore, aiming at predicting the XRS diagram for a multilayer, one should have the PSD information of all the layers.

Being impossible to directly measure the roughness of layers other than the substrate and the outermost layer, it is necessary to use a model to infer the PSDs of the inner layers. Physically, the roughness of the interface on top of each layer stems from two effects: the replication of the roughness of the underlying interface and the roughness introduced by the growth of the layer itself. A well-known multilayer growth model⁵ can be thereby used to describe the roughness evolution of the interfaces, as well as the correlation of the roughness between every pair of interfaces. We had already implemented this model in an IDL-based program⁶ aimed at reproducing the roughness evolution of several periodic multilayer coating samples, produced using different deposition techniques. The results were validated by the comparison of the XRS diagram, predicted from the roughness evolution, and the measured one at the standard X-ray energy of 8.045 keV (Cu-K α line), and at the 1st Bragg peak incidence angles. The model-to-data matching was very

good, but the analysis was limited to periodic multilayers. Multilayers for hard X-ray (> 10 keV) astronomy purposes, however, have a graded structure⁷. The accurate modeling of the XRS diagram one can expect from the surface topography of a multilayer is therefore interesting to estimate the impact on the PSF of a hard X-ray optical module.

In this work we extend the computation method from periodic to graded multilayers. The input data are still the measured PSD for the outermost layer and the substrate, mainly obtained from Atomic Force Microscopy (AFM), and the layer thickness values derived from the accurate fit of X-Ray reflectivity (XRR) measurements^{8,9}. A few growth parameters can be tuned for the growth analysis to fit the measured external PSD. When all those inputs are set, the internal PSDs for all the interfaces and the Crossed Spectral Densities for all the couples of interfaces can be reconstructed. Finally, aiming at checking the correctness of the growth description, we computed the expected XRS diagram from the modeled roughness growth, and compared it to the one measured at 8.045 keV with the BEDE-D1 diffractometer installed at INAF-OAB, at the incidence angle corresponding to the first reflectivity maximum after the critical angle. With respect to our previous work⁶, the main advance in the computation consisted of:

1. using the accurate film thickness trend instead of using the average d-spacing, d , and the high-Z thickness/d-spacing ratio, Γ , as in the periodic case,
2. extending the growth formalism to multilayers of variable instead of constant layer thickness values, and
3. adopting a more general method to compute the electric field trend throughout the multilayer stack, regardless of its periodicity.

In section 2 we describe the growth model⁵ that we implemented in the MPES program⁶, and the XRS formalism applied to multilayers. In section 3 we describe the samples and show the modeling results, as well as the predicted XRS Vs. the measurement. For the periodic case, we have re-analyzed the data already treated⁶, showing that including the modeled PSD growth and adopting the accurate electric field modeling leads to the best data/model matching. For the graded case, we show that the power law that describes the stack and fits the XRS peak positions is univocally determined, and also matches the XRR measurement. We demonstrate that the XRS diagram strongly depends on the electric fields calculation, and that the modeling of PSD evolution and electric field match the measured XRS. We finally show that surfacial defects on the sample, initially believed to be surface contamination, are enclosed in the stack and have to be included in the PSD in order to properly fit the XRS data. Results are briefly summarized in section 4.

2. MODELING MICROROUGHNESS GROWTH AND X-RAY SCATTERING IN MULTILAYERS

We hereafter summarize the adopted model⁵ to reproduce the roughness growth from the substrate layer to the external layer. This model had been already implemented⁶ in an IDL-based code, named MPES, and successfully tested for periodic multilayers.

For a single layer deposited over a substrate, the profile of this layer $z(x)$ can be described by a kinetic equation that considers a competition between a surface relaxation process and the increase in roughness due to the random nature of the deposition process (Eq. 1). These two actions are represented by the two terms on right-hand side:

$$\frac{\partial z(x)}{\partial \tau} = -\nu |\nabla^n z(x)| + \frac{\partial \eta}{\partial \tau} \quad (1)$$

In this equation, ν is a parameter that characterizes the relaxation process. The exponent n , is a positive integer varying with the kinetic mechanism that dominates the smoothing process⁵. In the second term, η is a random shot noise of the deposition process and accounts for the increase in roughness with the layer thickness τ . By solving Eq. 1 in terms of the surface PSD⁵ we obtain the intrinsic 2D-PSD of the layer surface, $P^{\text{int}}(f)$, i.e. the PSD that the surface layer would have if the substrate were ideally smooth:

$$P^{\text{int}}(f) = \Omega \frac{1 - \exp(-2\nu |2\pi f|^n \tau)}{2\nu |2\pi f|^n} \quad (2)$$

This PSD is characterized by a plateau up to the maximum frequency corresponding to the wavelength $l^* = (\nu\tau)^{1/n}$, then decreases as a power-law of spectral index n . Ω represents the volume of the deposited particle.

When we consider a multilayer, the situation is complicated by the presence of two elements with different properties, i.e., different values of the parameters Ω , ν , n . However, we can extend the formalism by considering each single layer (whose upper surface is labeled with $i = 0, 1 \dots 2N$ from the substrate to the surface) as growing upon its underlying layer, which acts as its “substrate”. In this way, we can write⁵ the PSD of the i^{th} interface as a sum of an intrinsic and an extrinsic part

$$P_i(f) = P_i^{\text{int}}(f) + P_i^{\text{ext}}(f) = P_i^{\text{int}}(f) + a_i(f)P_{i-1}(f) \quad (3)$$

where, in the extrinsic part, $a_i(f) = \exp(-\nu_i |2\pi f|^n \tau_i)$ is a replication factor that describes to which extent the microrelief components of the $(i-1)^{\text{th}}$ interface are replicated in the i^{th} layer. Like the P^{int} term, the replication factor exhibits a cutoff at the wavelength of $l^* = (\nu\tau)^{1/n}$, that represents the transition above which surface features are damped out. At wavelengths larger than l^* , the surface topography is almost entirely replicated. For periodic multilayers, the PSD of the outermost surface is easy to compute, since the recursive application of Eq. 3 leads to a geometric summation. In the case of graded multilayers, this is no longer possible and the Eq. 3 has to be applied iteratively to obtain the measured PSD. This increases the computation time and the search for the fitting values of parameters for the high- and low- Z density element Ω_h , ν_h , n_h , Ω_l , ν_l , n_l may become more intensive, but still on the order of a few hours with a commercially-available processor.

Typically, three different regimes of PSD evolution may be found:

1. the *low spatial frequency* regime ($l > 10 \mu\text{m}$), where the substrate PSD is replicated by every layer interface and the roughness is nearly conserved with a complete phase correlation;
2. the *intermediate spatial frequency* regime ($0.01 \mu\text{m} < l < 10 \mu\text{m}$), where the interfaces become progressively rougher than the substrate, owing to the partial replication of the underlying topography and the contribution of the layer growth;
3. the *high spatial frequency* regime ($l < 0.01 \mu\text{m}$), where the previously deposited layer features are damped out and the roughness is uncorrelated, i.e., not related in phase to the underlying layers.

In order to reconstruct the roughness evolution throughout the stack, we have measured the PSD of our samples with an Atomic Force Microscope (AFM) in the spatial wavelength range $0.005 \mu\text{m} < l < 10 \mu\text{m}$, for both the substrate and the outermost surface, in order to include the intermediate and the high frequencies regimes. Moreover, for the computation we used the layer thickness trend τ_i , which we derived by fitting the XRR measurements with the PPM program. Finally, for both the absorber and the spacer of the multilayer, we manually adjusted the three growth parameters Ω , ν , and n , until the outermost layer modeled PSD, obtained by recursive application of the Eq. 3, matched the experimentally measured PSD. Once the best-fitting parameter values are found, we use them to model the evolution of the PSD in the multilayer. Moreover, we are able to compute the cross correlations that are needed for the scattering computation⁶.

The independent proof of the correct modeling of the roughness growth comes from the X-ray scattering. The first order perturbation theory of the XRS in grazing incidence, assuming that the surface is smooth and isotropic, returns a relation between the roughness of the layer, described by its PSD, and the X-ray scattering diagram. For a single boundary, the relation is a simple proportionality^{1,2}. In the case of a multilayer, this relation is complicated by the interference effects of all the interfaces^{3,4}. For our purpose, we have used the following relation¹⁰

$$\begin{aligned} \frac{1}{I_0} \frac{dI_s}{d\theta_s} &= \frac{16\pi^2}{\lambda^3} Q_{is} \sin^2 \theta_s \sin \theta_i [P_{unc}(f) + P_{corr}(f)] = \\ &= \frac{16\pi^2}{\lambda^3} Q_{is} \sin^2 \theta_s \sin \theta_i \left[\sum_i T_i^2 P_i(f) + 2 \sum_{i>j} (-1)^{i+j} C_{ij}(f) T_i T_j \cos(\alpha \Delta_{ij}) \right] \end{aligned} \quad (4)$$

This formula allows us to directly compare the experimental XRS pattern (on left-hand side) to the theoretically predicted one, expressed in terms of spectral densities out of the roughness evolution model; P_i is the PSD of the i^{th} interface, C_{ij} is the Crosses Spectral Density of the i^{th} - j^{th} interface pair. I_0 is the incident flux, I_s the scattered intensity at the scattering angle θ_s , θ_i the grazing incidence angle, λ the wavelength of the incident radiation. Q_{is} is the polarization factor $Q_{is} = [R_F(\theta_s) R_F(\theta_i)]^{1/2}$, R_F the single boundary Fresnel reflectivity of the couple spacer/absorber of the multilayer, evaluated at the angles θ_s and θ_i . T_i is the amplitude transmittance in the j^{th} layer, i.e., $T_i = E_i/E_0$, E_0 the

electric field amplitude at the multilayer outer surface, $\alpha=2\pi/\lambda(\sin\theta_s+\sin\theta_i)$ is the perpendicular component of the scattering vector, and finally $\Delta_{ij}=\langle z_i \rangle - \langle z_j \rangle$ is the distance between the i^{th} and the j^{th} interface. Both incidence and scattering angles are corrected for internal refraction in the stack, which means that the formula can be used only for incidence angles larger than the critical angles of both materials.

Equation 4 can be applied to any multilayer at any incidence angle beyond the critical ones. In practice, to maximize the intensity of the scattered beam, it is convenient to set the incidence angle at the first peak after the critical angle. For a periodic stack, this is the 1st Bragg peak. The polarization factor Q_{is} is computed from Fresnel equations and the T_i coefficients are derived from the multilayer reflectivity. Two methods are used to compute T_i : the first one is applicable to periodic multilayers and assumes an exponential decrease of the intensity throughout the stack¹⁰ when rays impinge at the k^{th} Bragg peak. The second method is a generalization of the first one and it is applicable to both periodic and graded multilayers, and makes use of the recursive theory of reflectivity and transmittance in multilayers. We have validated the recursive method by comparing its results with the findings of the IMD program¹¹, for both periodic and graded samples. A good matching of outcomes of the two programs made us confident in using this method for computing the scattering. Finally, the result of Eq. 3 was added to a delta-like at $\theta_s = \theta_i$ to simulate the specular reflected beam and then degraded to the actual angular resolution of the detector (350 arcsec using a 400 μm wide slit).

3. EXPERIMENTAL RESULTS VS. MODELING

In this work we consider two samples as test cases:

- A) a periodic multilayer with $N = 40$ bilayers of W/Si with $d = 4.6 \text{ \AA}$ and $\Gamma = 0.42$ deposited by e-beam evaporation on a Si substrate (already characterized and analyzed⁶) and
- B) a graded multilayer with $N = 100$ bilayers of Pt/C deposited a few years ago by magnetron sputtering onto a Si substrate, with layer thicknesses as per the widespread supermirror design¹². The power-law parameters are provided in Tab. 1. Platinum is the first layer deposited onto the substrate and the outermost layer is in Carbon.

Table 1: main parameters of the analyzed samples

	Type of multilayer	Substrate	Number of bilayers	Absorber	Spacer	Layer thickness parameters (d and a in \AA)	Growth parameters Ω in nm^3 , l^* in nm
Sample A	Periodic	Si	40	W	Si	$d = 46$, $\Gamma = 0.42$	W: $\Omega = 24.46$ $l^* = 8.5$ n=5 Si: $\Omega = 0.02$ $l^* = 1.35$ n=3
Sample B	Graded	Si	100	Pt	C	Pt : $a = 31.0$ $b = -0.94$ $c = 0.23$ C: $a = 53.0$ $b = -0.88$ $c = 0.21$	Pt: $\Omega = 30.0$ $l^* = 10$ n = 5 C: $\Omega = 0.009$ $l^* = 2$ n = 2

Sample A

The complete characterization of this sample is already reported in a previous work⁶. The roughness growth was also studied in detail therein. The XRS scan, taken at the 1st Bragg peak, exhibits an apparent peak at $\theta_s = 10000$ arcsec, resulting from the constructive interference of scattered waves. We hereafter reconsider those data to validate the method used for the electric field calculation. Fig. 1 recapitulates the different possibilities we considered. In the first row we see the comparison between the measured XRS and the modeled curve when no roughness growth is assumed, i.e., when all the intermediate layers are assumed to have the same PSD as the external layer. The model clearly overestimates the experimental line. Computing the XRS using the more accurate recursive method improves the accord, but the model exhibits a small scattering peak at scattering angles close to 17000 arcsec that is not observed in the measured curve. When the PSD growth is accounted for, the agreement of the model to the data is improved and causes the additional peak to disappear. In particular, including the roughness evolution and adopting the recursive method for the electric fields returns a very performing fit of experimental data for the periodic case.

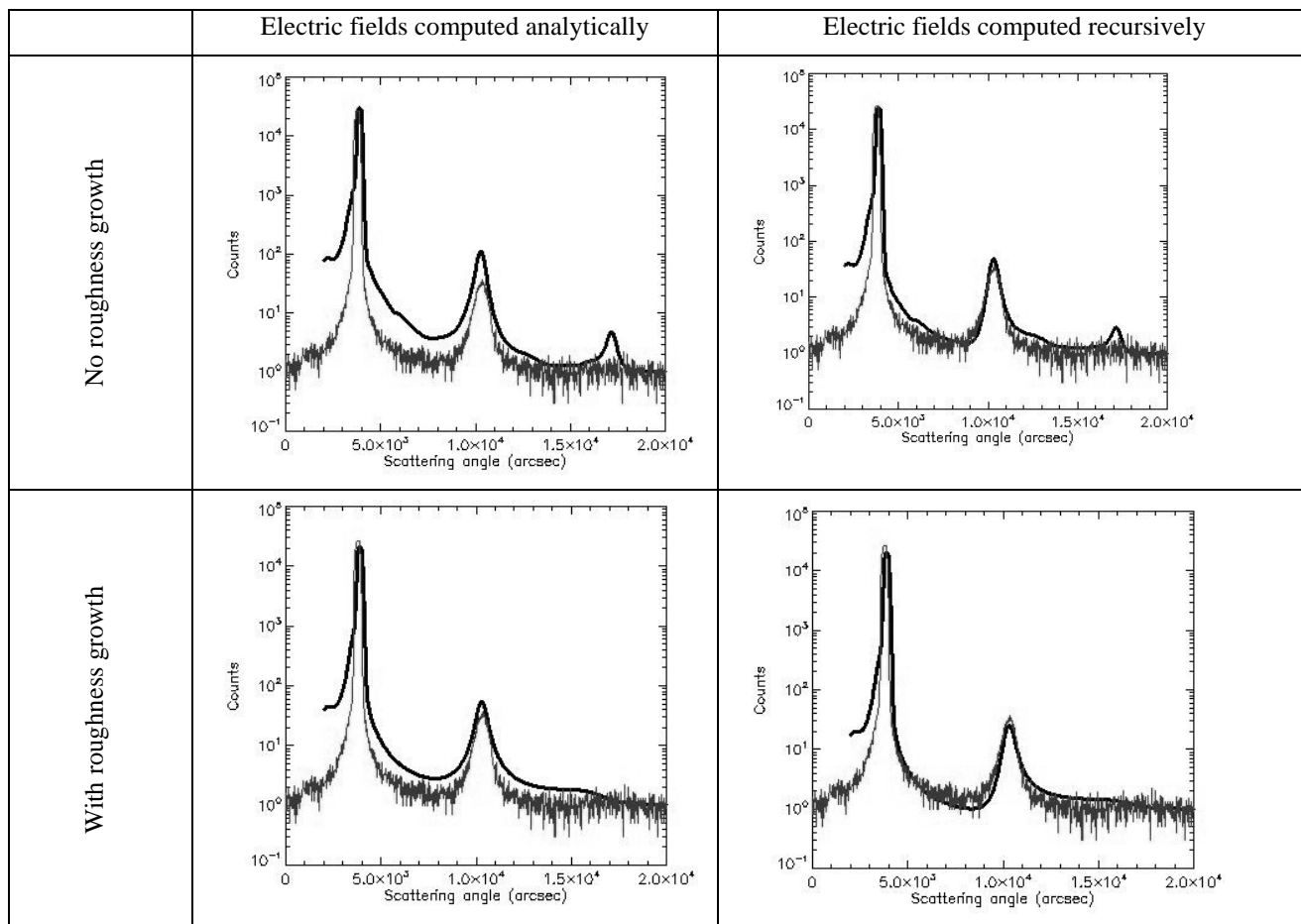


Fig. 1: X-ray scattering diagram for sample A. The modeling (black line) is compared to the experimental (red line). The best model-to-data matching is obtained assuming the complete roughness growth⁶ and adopting the more accurate recursive computation of electric fields.

Sample B

In order to characterize the roughness of this sample, we have performed AFM measurements of the outermost C layer surface in the 10-0.005 μm spatial wavelength range, while we assumed as substrate roughness the same of a Si wafer, in general close to a standard smoothness level¹³, e.g., a 2 \AA rms in the 10-0.05 μm spectral band. In contrast, the multilayer surface exhibits crowded point-like defects in ejection (Fig. 2): some defects of bigger size have the effect to increase the rms from 3.7 \AA to 7.3 \AA in the 10 μm scan range (see Tab. 2). Those defects are homogeneously present on the sample, but it is difficult to ascertain, by eye, if they are surfacial contaminations, inclusions in the multilayer or related to the roughness growth process. If they are dust contamination, they should not be accounted for in the PSD computation, whereas they should if they are the result of the roughness growth in the multilayer deposition process. In the latter case, those defects would be effective for X-ray scattering, whilst in the former one 8.045 keV X-rays would be almost unaffected by their presence. For this reason, we have performed two modeling of the roughness growth, including or excluding the surface defects seen with the AFM. The two roughness growth models have been used to simulate the XRS diagram at the standard X-ray energy of 8.045 keV, impinging on the sample at the first peak of reflectivity after the critical angle (2982 arcsec). The different PSD evolutions are shown in Figs. 4 through 6.

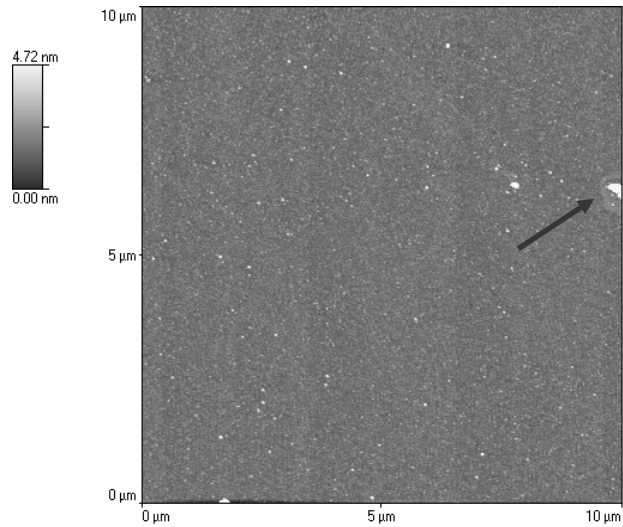


Fig. 2: a 10 μm wide AFM scan of the outer surface of sample B, the graded multilayer. The surface is crowded with point-like defects in ejection, and also exhibits some inclusions in the stack, likely Platinum crystals. The AFM measurement does not allow us distinguishing them from dust contaminations.

Table 2: experimental roughness for the outer surface of sample B in the 10 - 0.05 μm range, when the largest defects included in the stack are included in (CASE 1) or ruled out of the PSD (CASE 2). The surface rms is well reproduced by the model in both cases. The final rms loosely depends on the stack structure adopted (either fit A or B, see Tab. 3).

	rms[\AA] CASE 1 with defects	rms[\AA] CASE 2 without inclusions
AFM	7.3	3.7
Simulated growth, fit A	8.3	3.9
Simulated growth, fit B	8.8	3.9

Another point of concern, for both PSD evolution and XRS modeling, is the layer thickness in the stack. To this end, we performed XRR (X-ray Reflectivity) measurements at 8.045 keV by means of the BEDE-D1 diffractometer, prior to measure the XRS of the sample. The accurate fitting of XRR data (Fig. 3) using the PPM program [6] returns the best-fit power-law parameters for the stack (Tab. 4, fit A). We have used this thickness values to firstly model the roughness growth (Eqs. 2 and 3) and to subsequently simulate the XRS diagram (Eq. 4). The electric fields were computed using the recursive method, which is the only one applicable for a graded multilayer and already tested with the Sample A. Nevertheless, the XRS diagram simulated in this way, did not perfectly fit our XRS data (Fig. 4), since the peak positions did not match the measured ones.

The peak position mismatch denotes some departure of the actual thickness trend from the modeled one. We have found that a slightly different power law (Tab. 3, fit B) matches much better the scattering peak positions (Fig. 6), leaving the XRR measurement nearly unchanged (Fig. 3). This power-law actually returns layer thickness values that do not differ by more than 3 \AA from the first one, but in the outermost C layer, which turns out to be 15 \AA thicker. The XRR measurements actually matches both A and B power laws (Fig. 3): in fact, the specular reflectivity is a little sensitive to the thickness of the outer C layer, because most of the XRR curve features that guide the XRR fit are determined more by the multilayer internal structure than by the thickness of the capping layer. In contrast, the XRS is much more sensitive to the increased roughness generated by a thicker C layer. We therefore adopted the power law given by the fit B as the most correct one.

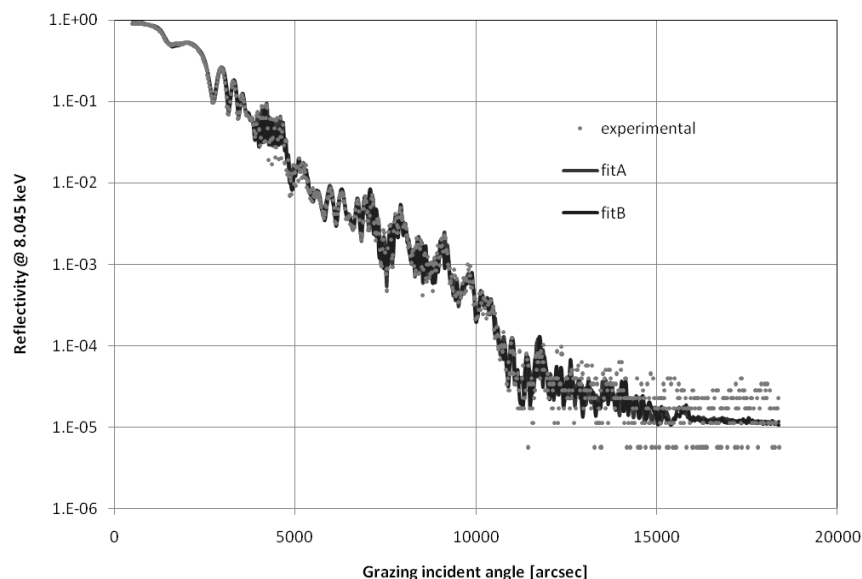


Fig. 3: XRR angular scan at 8.045 keV of sample B, compared to the best fit model calculated by PPM (fit A) and the power law used to fit the XRS measurement (fit B). The two models are nearly mutually undistinguishable by the sole XRR, but they yield a major difference in the XRS measure (Fig. 4 and 6).

Tab.3: power-law thickness parameters: fit A was found by fitting the sole XRR measurement, while fit B matches both XRR and XRS measurements

	Pt: a [Å], b , c	C: a [Å], b , c
Fit A	31.08, -0.90, 0.30	53.16, -0.96, 0.19
Fit B	31.00, -0.94, 0.23	53.00, -0.88, 0.21

The results of the roughness evolution modeling and the XRS diagrams computed from them, are presented in Figs. 4 through 6. From Fig. 5 we can see that, assuming the fit B for the power-law, the peak positions match the experimental ones. However, if the major defects are not included in the computation of the PSD, and in the consequent PSD evolution, the peak heights are underestimated in the simulated XRS diagram. Conversely, if the entire AFM maps are used to compute the final PSD of the multilayer and growth parameters are tuned accordingly, *the XRS diagram computed from the interfacial PSD and the cross correlation functions is in excellent accord with the experimental XRS curve* (Fig. 6). This provides not only an independent proof of the correct modeling of the roughness evolution throughout the stack, but also shows that large surface defects, though separated by several microns, are responsible for scattering X-rays. The XRS analysis also proves that the defects are actually resulting from the multilayer roughening and they are not related to a surfacial contamination by dust.

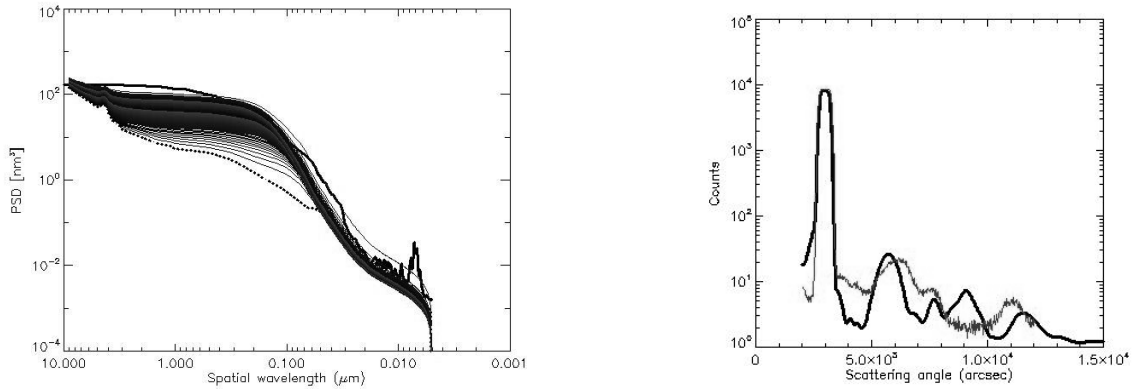


Fig. 4: (left) PSD evolution from the substrate (dotted line) to the outermost layer (thicker line) *including* large surface defects (CASE 1). Growth parameters: Pt: $\Omega=30.0$ $l^*=10$ $n=5$, C: $\Omega=0.009$ $l^*=2$ $n=2$. (right): experimental XRS for sample B (red line) compared with the simulated (black line) from the PSD evolution, computed with layer thickness fit A. The XRS graphs give evidence that the layer thicknesses, as determined by the XRR measurements, do not accurately fit XRS peak positions.

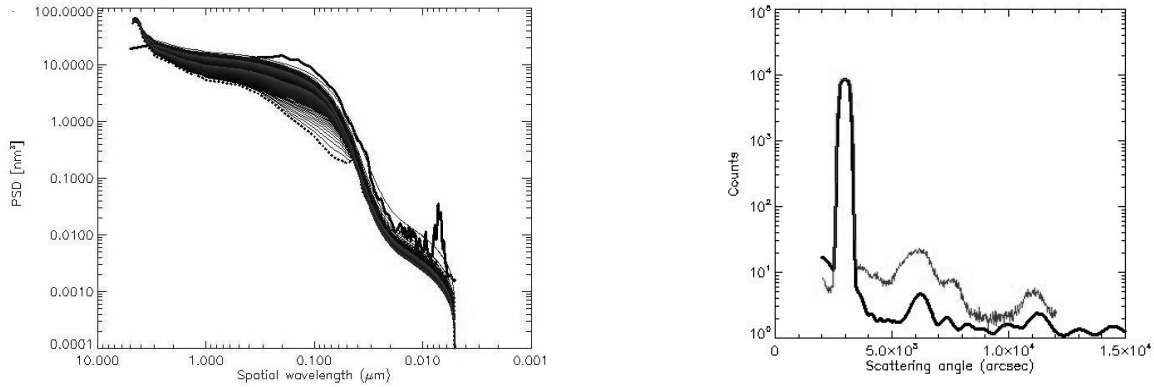


Fig. 5: (left): PSD evolution from the substrate (dotted line) to the outermost layer (thicker line) *excluding* large surface defects (CASE 2). Growth parameters: Pt: $\Omega=1.9$ $l^*=5.7$ $n=6$, C: $\Omega=0.009$ $l^*=2$ $n=2$. (right): experimental XRS for sample B (red line) compared with the simulated (black line) from the PSD evolution, computed with layer thickness fit B. This graph shows that different layer thicknesses (fit B) used to fit XRS peak positions are not sufficient to match XRS intensities when no included defects in the stack are considered (CASE 2).

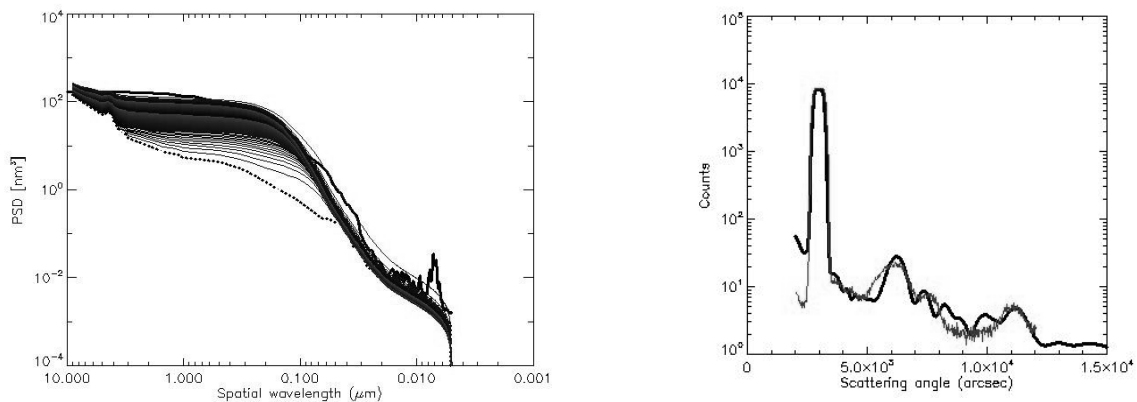


Fig. 6: (left): PSD evolution from the substrate (dotted line) to the outermost layer (thicker line) *including* large surface defects (CASE 1). Growth parameters: Pt: $\Omega=30.0$ $l^*=10$ $n=5$, C: $\Omega=0.009$ $l^*=2$ $n=2$. (right): experimental XRS for sample B (red line) compared with the simulated (black line) from the PSD evolution, computed with layer thickness fit B. *Including surface defects in the PSD evolution and the corrected layer thickness trend reproduced very well the measured XRS.*

4. CONCLUSIONS

We have shown that the study of the roughness evolution throughout a multilayer, so far⁶ limited by us to periodic multilayers, can be easily extended to graded ones. This also enables an XRS prediction, and an independent verification of the roughness growth modeling by comparison with the experimental measurement of the XRS diagram. In the tested cases we have reached a very good experiment-modeling simultaneous matching for both PSD growth and X-ray scattering. In particular, we have proven that assuming the correct roughness evolution in the stack is crucial to return correct results in terms of XRS. Moreover, we have shown that the XRS diagram for graded multilayers is even more sensitive than an XRR measurement, though accurately fitted, to the actual thickness trend in the stack since even a few angströms variation significantly changes the XRS peak positions. Finally, we have shown that the defects seen in the AFM map are included in the stack because they produce X-ray scattering levels that would not be reproduced by ruling them out of the PSD evolution. This example demonstrates the power of the XRS as a diagnostic instrument, provided that it is coupled to an opportune modeling of the PSD evolution in multilayers and that the XRS pattern can be reliably modeled (Eq. 4).

Future developments of this work will be aimed to continue the validation of the methodologies and the IDL codes with a larger number of graded multilayer samples.

ACKNOWLEDGMENTS

This work has been financed by the Italian Space Agency (contract I/069/09/0).

REFERENCES

- [1] Stover, J.C., "Optical scattering: measurement and analysis", SPIE Optical Engineering Press, (1995)
- [2] Church, E. L., Takacs, P. Z., "Interpretation of grazing incidence scattering measurements", Proc. SPIE 640, 126 - 133, (1986)
- [3] Holy, V., Pietsch, U., Baumbach, T., "High resolution X-ray scattering from thin films and multilayers" Springer, Berlin, (1999)
- [4] Kozhevnikov, I.V., "Analysis of X-ray scattering from a rough multilayer mirror in the first-order perturbation theory", Nuclear Instruments and Methods in Physics Research A498, 482 - 495, (2003)
- [5] Stearns, D.G., Gaines, D.P., Sweeney, D.W., Gullikson, E.M., "Nonspecular x-ray scattering in a multilayer-coated imaging system", Journal of Applied Physics, 84, 1003-1028, (1998)
- [6] Canestrari, R., Spiga, D., Pareschi, G., "Analysis of microroughness evolution in X-ray astronomical multilayer mirrors by surface topography with the MPES program and by X-ray scattering", Proc. SPIE 6266, 626613, (2006)
- [7] Y. Tawara, K. Yamashita, H. Kunieda, et al., "Development of a multilayer supermirror for hard x-ray telescopes" SPIE Proc. 3444, 569 - 575 (1998)
- [8] Spiga, D., Mirone, A., Pareschi, G., Canestrari, R., Cotroneo, V., Ferrari, C., Ferrero, C., Lazzarini, L., Vernani, D., "Characterization of multilayer stack parameters from x-ray reflectivity data using the PPM program: measurements and comparison with TEM results", Proc. SPIE 6266, 626616, (2006)
- [9] Spiga, D., Pareschi, G., Cotroneo, V., Canestrari, R., Mirone, A., Ferrero, C., Ferreari, C., Lazzarini, L., and Vernani, D., "Multilayer coatings for X-ray mirrors: extraction of stack parameters from x-ray reflectivity scans and comparison with transmission electron microscopy results", Optical Engineering, 46(8), 086501 (2007)
- [10] Spiga, D., "Development of multilayer-coated mirrors for future X-ray telescopes", PhD thesis, Università di Milano Bicocca, (2005)
- [11] Windt, D.L., "IMD-Software for modeling the optical properties of multilayer films", Computer in Physics, 12, 360-370, (1998)
- [12] Joensen, K. D., Voutov, P., Szentgyorgyi, A., et al., "Design of grazing-incidence multilayer supermirrors for hard X-ray reflectors", Applied Optics, 34(34), 7935-7944, (1995)
- [13] Vernani, D., Pareschi, G., Mazzoleni, F., Spiga, D., Valtolina, R., "Surface characterization of superpolished substrates for X-ray and neutron multilayer optics" Materials Structure, 13(2), 71-75 (2006)